Picosecond acoustics in p-doped piezoelectric semiconductors

P. Babilotte, P. Ruello,[a] G. Vaudel, T. Pezeril, D. Mounier, J.-M. Breteau, and V. Gusev[b]
Laboratoire de Physique de l'Etat Condensé, UMR CNRS 6087, Université du Maine, 72085 Le Mans, France

(Received 20 May 2010; accepted 22 September 2010; published online 27 October 2010)

We demonstrate by experiment and theoretical analysis that the presence of built-in electric fields near the (111) and $(\bar{1}\bar{1}\bar{1})$ surfaces of p-doped GaAs causes efficient generation of acoustic waves due to the laser-induced inverse piezoelectric effect. At the same time, the generation efficiency from the electron-hole-phonon deformation potential is shown to be reduced. The polarity of the acoustic pulse is inverted when changing the laser irradiated surface from (111) to $(\bar{1}\bar{1}\bar{1})$. The results have ramifications for optically controlled piezoelectric ultrasound transducers. © *2010 American Institute of Physics*. [doi:10.1063/1.3501125]

Laser-based picosecond ultrasonics[1] is an important tool for the nondestructive evaluation of nanostructures and nanomaterials.[2] Different physical mechanisms for optoacoustic conversion have been studied with the goal of increasing the efficiency in the conversion of femtosecond laser pulses into acoustic strain.[1,3–10] Piezoelectric generation is driven by transient depolarising electric fields created by the spatial separation of electrons and holes following interband absorption of optical radiation in piezoelectric semiconductors.[3,6–9] A recent investigation found a sublinear growth of photoinduced picosecond strain at high fluence, indicating that acoustic generation in piezoelectric semiconductors starts to diminish in efficiency when the laser fluence is increased.[9] Here we demonstrate that, in a generic sample of p-doped ⟨111⟩ GaAs, the sublinear growth is followed by complete saturation, that is, by a "plateau," in the dependence of picosecond strain amplitude on laser fluence. This result is reproduced theoretically by a model revealing the importance of the depth of the near-surface depletion zone.

Our ultrafast pump-probe testing of the transient reflectivity of ⟨111⟩ GaAs is conducted with deeply penetrating red probe radiation (laser pulse duration $\tau_L \approx 200$ fs, wavelength $\lambda_r \approx 790$ nm, and penetration depth $\alpha_r^{-1} \approx 800$ nm), that is, we operate under conditions of so-called picosecond ultrasonic interferometry.[1] The collinear pump and probe beams at normal incidence have approximately equal diameters d of 20 μm at the $1/e^2$ intensity level. The dominant contribution to the acoustically induced part of the transient reflectivity $\Delta R/R$ is a damped sinusoidal oscillation (see inset in Fig. 1) at the Brillouin frequency ω_B, which is determined by momentum and energy conservation in the photon–phonon interaction. For normal incidence of the probe pulses on the sample, the frequency of the detected ultrasound is $\omega_B = 2k_r' v_a \approx 3 \times 10^{11}$ s^{-1}, where k_r' is the real part of the probe light wave number in GaAs and $v_a \cong 5.4 \times 10^3$ m/s is the speed of longitudinal waves in the [111] direction of GaAs. The Brillouin oscillation is described by[1,10] $\Delta R/R \propto \mathrm{sgn}(\partial k_r'/\partial \eta)\mathrm{Re}[i\tilde{\eta}^*(\omega_B)\exp(i\omega_B t)]$, where $\tilde{\eta}(\omega_B)$ is the component of the generated acoustic strain at the Brillouin frequency.

We use p-type GaAs:Zn, with an equilibrium majority-carrier (hole) concentration of $n_{h0} = 3.1 \times 10^{17}$ cm^{-3}, grown in the [111] direction corresponding to the maximum magnitude of the piezoelectric modulus ($p_E = 2p_{14}/\sqrt{3} \approx 0.185$ C/m^2). Results for blue pump radiation ($\lambda_b \approx 395$ nm and $\alpha_b^{-1} \approx 14$ nm) are shown in Fig. 1. The growth of the amplitude of the transient reflectivity signal at the Brillouin frequency ω_B completely saturates above the critical pump laser fluence F_L of ≈ 5 μJ/cm^2 and the plateau persists up to the maximum fluence F_L of ≈ 15 μJ/cm^2. The Brillouin oscillations corresponding to opposite faces of the sample are in antiphase (see inset in Fig. 1) and can be fitted at faces A and B over the complete observation range by the function $\Delta R/R \propto \pm\cos(\omega_B t)$, respectively, where $t=0$ corresponds to the arrival time of the pump pulse at the surface. The existence of the plateau seems at first surprising, because in a transition from the efficient strain generation via the inverse piezoelectric effect to the less efficient generation via the deformation-potential effect, a continuous growth in the ultrasound amplitude might have been expected.[8]

We interpret these experimental results by theoretical modeling of the processes of ultrasound generation and using appropriate quantitative estimates. The laser-induced mechanical stress exciting acoustic waves in GaAs can be approximated by a sum of the piezoelectric stress $\sigma_{\mathrm{piezo}} = -p_E \Delta E$, and the stress due to electron-hole-phonon deformation potential $\sigma_{e+h} = -d_e \Delta n_e - d_h \Delta n_h$, where $\Delta E(t,z)$ and $\Delta n_{e,h}(t,z)$ are the laser-induced transient modifications in the

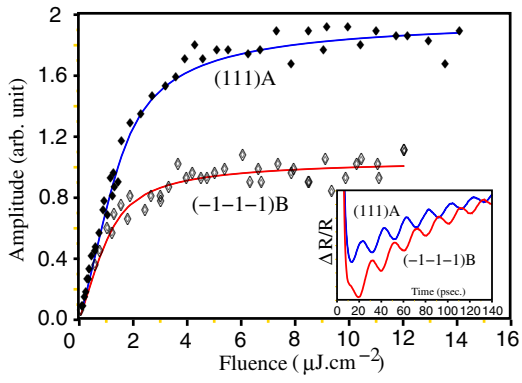

FIG. 1. (Color online) Dependence of the Brillouin oscillation amplitude on the fluence F_L of the blue pump pulse measured (diamonds) and theoretically fitted (curves) at opposite faces of the p-doped ⟨111⟩ GaAs. Inset: The antiphase Brillouin oscillations in transient reflectivity signal at opposite faces of the sample.

[a]Electronic mail: pascal.ruello@univ-lemans.fr.
[b]Electronic mail: vitali.goussev@univ-lemans.fr.

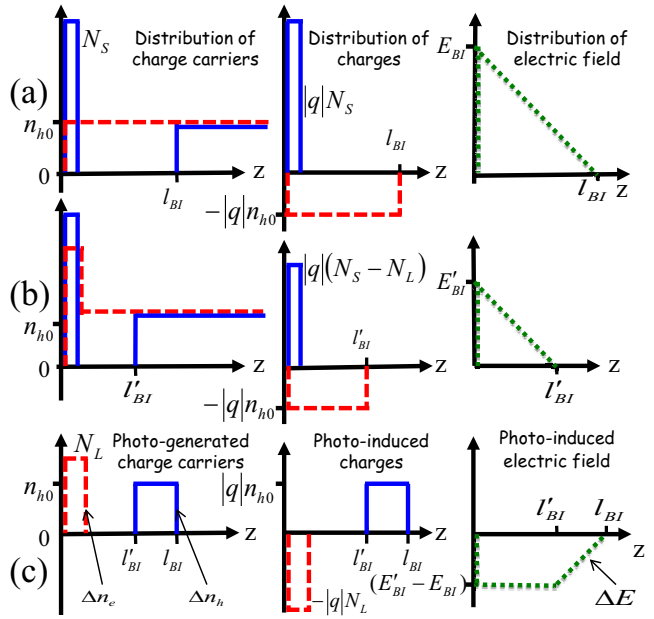

FIG. 2. (Color online) In-depth distributions of electrons and holes concentrations (left column), of the electrical charge concentrations (middle column) and of the electric field (right column) in the p-doped GaAs before [$t=0^-$, row (a)] and after [$t\geq 0^+\approx 3$ ps, row (b)] the arrival of the femtosecond pump laser pulse. [Row (c), $t\geq 0^+$]: The distributions of photogenerated carriers and charges and of the photoinduced depolarising electric field. The distributions of holes and positive charges, of electrons and negative charges, and of the electric field are presented by continuous, dashed, and dotted lines, respectively.

distributions of the electric fields and the concentrations of the electrons (holes), $d_e\approx 7.17$ eV and $d_h\approx 1.16$ eV are the deformation potentials of electrons and holes,[11] and z is the coordinate axis along the inward normal to the semiconductor surface. The thermoelastic contribution to the laser-generated ultrasound is known to be negligible in GaAs.[3,5] The laser action can be considered as instantaneous at $t=0$ because the laser pulse duration is significantly shorter than the period of the Brillouin oscillation $T_B=2\pi/\omega_B\approx 20$ ps. To model the transient ΔE and $\Delta n_{e,h}$ we start with the presentation in Fig. 2 [row (a)] concerning the distributions of carrier concentrations, of charge concentrations and of the built-in electric field at time $t=0^-$ just before the arrival of the laser pulse. These are the majority carriers that are providing the net charge to the surface,[12] so both surfaces of the p-doped GaAs are positively charged at $t=0^-$, and Fig. 2 is valid for both faces of GaAs. We present the distributions of carrier concentration and of the related charge near the surface $z=0$ by rectangular functions of finite width. The width of these distributions is much narrower than the width of the zone $0\leq z\leq l_{BI}(t=0^-)\equiv l_{BI}$ that is depleted of holes and possessing homogeneously distributed negative charge density equal to $-|q|n_{h0}$ because of the strong inequality $|q|V_{BI}\approx 0.5$ eV $\gg k_BT_{\text{room}}\cong 0.026$ eV between the built-in potential and the thermal energy in p-doped GaAs.[13] Here $|q|=1.6\times 10^{-19}$ C is the elementary charge, k_B is the Boltzmann constant, and T is the temperature. The knowledge of the built-in potential and of the doping concentration leads to estimates[13,14] of all the parameters in the depletion zone presented in Fig. 2 [row (a)]; the sheet concentration of elementary charges (holes) at the surface $N_S(t=0^-)\equiv N_S\cong\sqrt{2\varepsilon\varepsilon_0 n_{h0}V_{BI}/|q|}\approx 1.5\times 10^{12}$ cm^{-2} lies inside the range $10^{11}-10^{13}$ cm^{-2} of commonly observed surface charge densities;[14] the depletion depth is $l_{BI}\cong N_S/n_{h0}\approx 50$ nm and the initial surface value of the built-in electric field is $|E_{BI}|\cong|q|N_S/(\varepsilon\varepsilon_0)\approx 210$ kV/cm. In the above formulas ε_0 is the dielectric permittivity of the vacuum and $\varepsilon\approx 13$ is the relative quasistatic dielectric permittivity of GaAs.

The pump laser pulse is absorbed at the depth $\alpha_b^{-1}\approx 14$ nm$<l_{BI}$, injecting in the depletion region equal sheet densities of electrons and holes $N_L=(1-R_b)F_L/(h\nu_b)$, where $R_b\approx 0.47$ and $h\nu_b$ are the reflectivity at the air/GaAs interface and the photon energy of the pump blue radiation. The photogenerated electrons are attracted by the surface while the holes are repelled. The charges separate due to their acceleration and drift in the built-in electric field. Their spatial distribution evolves later, by the combined effects of drift and diffusion, to the quasiequilibrium form presented in Fig. 2 [row (b)] where $l'_{BI}=(1-N_L/N_S)l_{BI}$ and $E'_{BI}=(1-N_L/N_S)E_{BI}$. It is this separation of charges that results in the reduced sheet concentration of surface charges N_S-N_L that induces the transient electric field—opposite in direction to the built-in field—that partially screens the latter. The detailed numerical estimates (not reproduced here) demonstrate that the time for complete screening of initial electric field when $N_L\geq N_S$ does not exceed 3 ps$\ll T_B$. The photoinduced transition from the equilibrium distribution of carriers, charges and fields presented in Fig. 2 [row (a)] to their quasiequilibrium distributions in Fig. 2 [row (b)] can be assumed instantaneous. We have termed the distributions at $t=0^+$ in Fig. 2 [row (b)] a "quasiequilibrium distributions" because the relaxation time of these distributions is much longer than the Brillouin period. The relaxation is long because relatively slow bulk recombination processes in GaAs (Ref. 4) are additionally suppressed by the spatial separation of photogenerated electrons and holes, whereas the carrier motion along the laser irradiated surface is suppressed by the quasi-one-dimensional character of the e-h photoinjected distributions.

Photoinduced variations in the distributions $\Delta E(t,z)$ and $\Delta n_{e,h}(t,z)$ can thus be obtained by taking the difference between the quasiequilibrium distributions corresponding to the final (N_s-N_L) and the initial N_s sheet densities of the surface charges, that is, by taking the difference of the rows (b) and (a) in Fig. 2. The resulting distributions presented in row (c), when substituted in the formulas for laser-induced stress, should be multiplied by the Heaviside step function $H(t)$ to account for the temporal dynamics. The solution of the acoustic wave generation problem near the mechanically free surface subject to the assumed photoinduced stresses provides[3] a description of the ultrasonic strain wave at the Brillouin frequency outside the generation region:

$$\tilde{\eta}_{\text{piezo}}(\omega_B)\cong\frac{qp_En_{h0}}{\varepsilon\varepsilon_0\rho v_a}\frac{1}{(i\omega_B^2)}[\gamma-\gamma'+\sin\gamma'-\sin\gamma], \quad (1)$$

$$\tilde{\eta}_{e+h}(\omega_B)\cong-\frac{d_hn_{h0}}{\rho v_a^2}\frac{1}{(i\omega_B)}[\cos\gamma'-\cos\gamma]. \quad (2)$$

Here ρ is the density of GaAs and $\gamma'\equiv(1-N_L/N_S)\gamma$, where $\gamma\equiv(\omega_B/v_a)l_{BI}$. These solutions predict that both generation of the acoustic signal by the inverse piezoelectric effect and the generation by the deformation potential saturate $(\partial\tilde{\eta}_{e=h}/\partial N_L=\partial\tilde{\eta}_{\text{piezo}}/\partial N_L=0)$ when the pump laser fluence F_L reaches the critical value F_{sat} necessary to inject the sheet

concentration of the electrons N_L equal to initial surface concentration N_s of holes $N_L(F_L=F_{sat})=N_s$. These solutions in Eqs. (1) and (2) imply that the ratio $|\tilde{\eta}_{piezo}/\tilde{\eta}_{e+h}|$ diminishes from ~250 to 50 when F_L increases from $F_L=0$ to $F_L=F_{sat}$; thus the piezoelectric optoacoustic conversion strongly dominates. This is partially due to the relatively large difference in the deformation potential of electrons and of holes,[11] $d_e/d_h \approx 6.2$ and the fact that the photoinjected electrons, localized much closer to the surface than the photoinjected holes, give a negligible contribution to sound generation because of the destructive interference between the wave emitted by them directly into the bulk and the wave emitted in the direction of the surface (and reflected by the free surface). The different functional dependences of $\tilde{\eta}_{piezo}$ and $\tilde{\eta}_{e+h}$ on γ and γ' indicate the importance of the difference in structure of the spatial distributions $\Delta E(t,z)$ and $\Delta n_{e,h}(t,z)$ inside the depletion region (see Fig. 2) in the interference of the generated acoustic waves. In particular, the closeness of the nondimensional parameter $\gamma \equiv (\omega_B/v_a)l_{BI}$ to π in our experiments contributes to the dominance of the inverse piezoelectric effect at low fluencies $F_L \ll F_{sat}$, in which case $|\tilde{\eta}_{piezo}/\tilde{\eta}_{e+h}| \propto (1-\cos\gamma)/\sin\gamma$.

For quantitative comparison with the experimental data, one must consider the predicted saturation of the signal at $F_L=F_{sat}$ across the profile of the pump beam. We substitute in Eq. (1) $N_L=N_L(r)=(1-R_b)F_L \exp[-2(2r/d)^2]/(h\nu_b)$, when $N_L(r) \le N_S$, and $N_L=N_S$, when $N_L(r) \ge N_S$, where r is the radial coordinate. Multiplying Eq. (1) additionally by the probe intensity distribution $\propto \exp[-2(2r/d)^2]$ and integrating over the laser-irradiated surface, we obtain,

$$\left|\frac{\Delta R}{R}\right| \propto \begin{cases} \dfrac{\gamma-\gamma'}{2} - \dfrac{\cos\gamma - \cos\gamma'}{\gamma-\gamma'} - \sin\gamma, \\ \dfrac{\gamma(\gamma-2\gamma')}{2(\gamma-\gamma')} - \dfrac{\cos\gamma - 1}{\gamma-\gamma'} - \sin\gamma, \end{cases} \tag{3}$$

for $N_L \le N_s$ and $N_L \le N_s$, respectively. The theoretical solutions in Eq. (3) have been fitted to the experimental data in Fig. 1 using vertical scaling and a single free parameter N_S controlling the shape of the saturation curves. The extracted concentrations of the surface charges at faces A and B are $N_S \approx 2.2\times10^{12}$ cm^{-2} and $N_S \approx 1.8\times10^{12}$ cm^{-2}, respectively.

In addition to the correct saturation behavior Eq. (1) predicts that $\Delta R/R \propto -\mathrm{sgn}(\partial k_r'/\partial\eta)\mathrm{sgn}(q)\mathrm{sgn}(p_E)\cos(\omega_B t)$. Taking into account that in p-doped GaAs $q>0$ for the holes and the photoelastic constant is positive for the used red probe light ($\partial k_r'/\partial\eta > 0$),[15] the phase of the Brillouin oscillation is controlled by the sign of the piezoelectric modulus. Thus the opposite phases of the Brillouin signal found for opposite faces of the sample (inset in Fig. 1) result from the third rank tensor of piezoelectric modules, which changes sign when the orientation of the z-axis changes from [111] to $[\bar{1}\bar{1}\bar{1}]$. Moreover, taking into account that the piezoelectric constant is negative for the face A ($p_E<0$) (Ref. 16) and positive for the face B ($p_E>0$) (Ref. 16) the developed theory correctly predicts the phases of the Brillouin signal observed in the experiment.

At pump fluence $F_L > F_{sat}$, fluence $F_L - F_{sat} > 0$ is absorbed in a semiconductor without a depletion region. It can therefore be expected that the e-h pairs generated by $F_L - F_{sat} > 0$ will exhibit the usual ambipolar diffusion. Estimates[3,5,10] demonstrate that for the case of GaAs excited by femtosecond blue laser pulses, the generation of the Brillouin signal by the deformation potential mechanism dominates the piezoelectric generation by the Dember electric field. For blue pump radiation ($\alpha_b > \omega_B/v_a > \sqrt{\omega_B/D_a}$) one finds,[3,10]

$$|\tilde{\eta}_{eh}(\omega_B)| \cong \frac{d_{e+h}}{\rho v_a^2}\frac{1}{\omega_B}\left(\frac{v_D}{D_a}\right) \times \left[1+\frac{S}{\alpha D_a}\right]\frac{(N_L-N_S)H(N_L-N_S)}{\sqrt{1+\sqrt{2}S/v_D+(S/v_D)^2}}, \tag{4}$$

where $d_{e+h}=d_e+d_h$, $D_a=(3-13)\times10^{-4}$ m^2/s (Ref. 5) is the ambipolar diffusivity, $v_D=\sqrt{D_a\omega_B} > v_a$ is the supersonic velocity of the diffusion wave at the Brillouin frequency and S is the surface recombination velocity. The comparison of the amplitude of the signal (4), evaluated at $N_L > N_S$, with the amplitude of the signal (1), evaluated at $N_L \ge N_S$, provides $|\tilde{\eta}_{piezo}(\omega_B)/\tilde{\eta}_{e+h}(\omega_B)| \approx 10N_S/(N_L-N_S)$. This estimate predicts that $|\tilde{\eta}_{e+h}(\omega_B)|$ becomes comparable with $|\tilde{\eta}_{piezo}(\omega_B)|$ only when $F_L - F_{sat} \ge 10F_{sat}$. This explains why there is no a visible continuous increase in the acoustic signal with increasing pump laser fluence and the plateau persists from $F_L \approx 5$ μJ/cm^2 up to $F_L \approx 15$ μJ/cm^2 in Fig. 1.

In conclusion, both experimental and theoretical findings in p-doped GaAs highlight the importance to the design of optically-driven piezoelectric ultrasonic antennas of the dimensionless parameter $\gamma \equiv (\omega_B/v_a)l_{BI}=k_B l_{BI}$, equal to the product of the wave number of the acoustic wave at the Brillouin frequency k_B and the width of the depletion zone l_{BI}. This parameter influences both the maximum efficiency of the optoacoustic generation and its saturation level.

This research has been conducted in the frame of the project "gigahertz optically controlled piezoelectrical transducers" of ANR BLAN program.

[1] C. Thomsen, H. T. Grahn, H. J. Maris, and J. Tauc, Phys. Rev. B **34**, 4129 (1986).
[2] J.-F. Robillard, A. Devos, and I. Roch-Jeune, Phys. Rev. B **76**, 092301 (2007).C. Mechri, P. Ruello, J. M. Breteau, M. R. Baklanov, P. Verdonck, and V. Gusev, Appl. Phys. Lett. **95**, 091907 (2009).
[3] S. A. Akhmanov and V. E. Gusev, Sov. Phys. Usp. **35**, 153 (1992); V. Gusev, Phys. Status Solidi B **158**, 367 (1990).
[4] O. Wright and V. Gusev, Appl. Phys. Lett. **66**, 1190 (1995).
[5] O. B. Wright, B. Perrin, O. Matsuda, and V. E. Gusev, Phys. Rev. B **64**, 081202 (2001).
[6] C.-K. Sun, J.-C. Liang, and X.-Y. Yu, Phys. Rev. Lett. **84**, 179 (2000).
[7] K.-H. Lin, C.-T. Yu, Y.-C. Wen, and C.-K. Sun, Appl. Phys. Lett. **86**, 093110 (2005).
[8] O. Matsuda, O. B. Wright, D. H. Hurley, V. E. Gusev, and K. Shimizu, Phys. Rev. Lett. **93**, 095501 (2004).
[9] Y.-C. Wen, L.-C. Chou, H.-H. Lin, V. Gusev, K.-H. Lin, and C.-K. Sun, Appl. Phys. Lett. **90**, 172102 (2007).
[10] V. Gusev, Acust. Acta Acust. **82**, S37 (1996).
[11] S. L. Chuang, *Physics of Optoelectronic Devices* (Wiley, New York, 1995).
[12] W. Monch, *Semiconductor Surfaces and Interfaces* (Springer, Berlin, 1993).
[13] S. M. Sze, *Physics of Semiconductor Devices* (Wiley, New York, 1981).
[14] K. Seeger, *Semiconductor Physics. An Introduction* (Springer, Berlin, 1982).
[15] F. Hudert, A. Bartels, T. Dekorsy, and K. Kohler, J. Appl. Phys. **104**, 123509 (2008).
[16] R. M. Martin, Phys. Rev. B **5**, 1607 (1972).